Neuroblastoma: Functional Imaging

19

Susan E. Sharp, Michael J. Gelfand, and Barry L. Shulkin

Neuroblastoma, ganglioneuroblastoma, and ganglioneuroma are tumors derived from primitive neural crest cells of the sympathetic nervous system. Neuroblastoma and ganglioneuroblastoma are usually grouped together for clinical purposes as both contain undifferentiated neuroblasts with malignant or potentially malignant behavior. In contrast, ganglioneuroma is a benign tumor containing only mature ganglion cells and other mature tissues [1].

Neuroblastoma is the most common extracranial solid tumor of childhood, comprising approximately 8 % of pediatric cancers. Median age at diagnosis is 15 months, with the vast majority of patients presenting during infancy or early childhood [2].

S.E. Sharp, MD (✉)
Department of Radiology,
Cincinnati Children's Hospital Medical Center,
University of Cincinnati College of Medicine,
Cincinnati, OH, USA
e-mail: susan.sharp@cchmc.org

M.J. Gelfand, MD
Section of Nuclear Medicine,
Department of Radiology,
Cincinnati Children's Hospital Medical Center,
Cincinnati, OH, USA

B.L. Shulkin, MD, MBA
Division of Nuclear Medicine,
Department of Radiological Sciences,
St. Jude Children's Research Hospital,
Memphis, TN, USA
e-mail: barry.shulkin@stjude.org

Neuroblastoma can arise anywhere along the sympathetic chain. Primary tumors most commonly occur in the adrenal gland (35 %), retroperitoneum (30–35 %), or posterior mediastinum (20 %) with pelvic and cervical primary sites less frequently seen (<5 %), respectively. Neuroblastoma rarely can present with metastatic disease without an identifiable primary tumor [1].

Metastatic disease is seen in more than half of neuroblastoma patients at diagnosis. Bone marrow and cortical bone are the most frequent metastatic sites, with lymph node and hepatic metastases also commonly seen. Lung and central nervous system metastases are rare and associated with very poor outcomes [3].

Neuroblastoma is staged using the International Neuroblastoma Staging System (INSS) which was developed in 1988 and revised in 1993 as summarized in Table 19.1 [4]. Presurgical staging of localized disease cannot be performed using the INSS, as staging is based on the extent of tumor resection and surgical assessment of lymph node involvement.

In 2009, the International Neuroblastoma Risk Group Staging System (INRGSS) was described, allowing presurgical staging of localized tumors as summarized in Table 19.2 [5]. The INRGSS uses imaging-defined risk factors to help predict surgical risk and surgical outcome [5–7]. The INRGSS also raises the age cutoff for the special stage used in infants with distant metastatic involvement limited to liver, skin, and/or bone marrow. This change reflects recent literature which suggests that a cutoff of 18 months more

S.T. Treves (ed.), *Pediatric Nuclear Medicine and Molecular Imaging*,
DOI 10.1007/978-1-4614-9551-2_19, © Springer Science+Business Media New York 2014

Table 19.1 Summary of the International Neuroblastoma Staging System (INSS)

Stage	Description
1	Localized tumor with complete gross excision. Negative ipsilateral lymph nodes (unless adherent to and removed with the tumor)
2A	Localized tumor with incomplete gross excision. Negative nonadherent ipsilateral lymph nodes
2B	Localized tumor with or without complete gross excision. Positive nonadherent ipsilateral lymph nodes
3	Unresectable tumor infiltrating across the midline with or without positive regional lymph nodes, localized unilateral tumor with positive contralateral lymph nodes, or midline tumor with bilateral extension by infiltration or lymph node involvement
4	Any primary tumor with distant metastatic disease (except stage 4s)
4s	Localized primary tumor (as defined by stage 1, 2A, or 2B) with distant metastatic disease limited to the skin, liver, and/or bone marrow in patients less than 12 months of age

From Brodeur et al. [4]. Reprinted with permission. Copyright 1993 American Society of Clinical Oncology. All rights reserved

Table 19.2 Summary of the International Neuroblastoma Risk Group Staging System (INRGSS)

Stage	Description
L1	Localized tumor without image-defined risk factors[a] and confined to one body compartment[b]
L2	Locoregional tumor with one or more image-defined risk factors[a]
M	Distant metastatic disease (except stage MS)
MS	Distant metastatic disease confined to skin, liver, and/or bone marrow in patients less than 18 months of age

From Monclair et al. [5]. Reprinted with permission. Copyright 2009 American Society of Clinical Oncology. All rights reserved

[a]Imaging defined risk factors include, but are not limited to, encasement of major vascular structures and invasion of adjacent organs

[b]Body compartments include the neck, chest, abdomen, and pelvis. Contiguous disease involvement of more than one body compartment (e.g., upper abdominal tumor with positive ipsilateral inferior mediastinal lymph nodes) would make a patient stage L2

accurately predicts outcome [8–12]. The INRGSS is meant to be used in conjunction with, but not replace, the INSS [5, 6].

The prognosis of neuroblastoma is widely variable. Some neuroblastomas spontaneously regress or mature without therapy, while others progress to widespread and fatal disease in spite of intensive multimodality therapy [8, 13, 14]. Neuroblastoma patients are divided into risk groups to guide therapy and predict outcomes. Risk groups are based on stage, age, and biologic tumor factors (such as histology, DNA ploidy, and MYCN amplification) [8, 13, 15].

Low-risk disease is treated with surgery or supportive care alone with survival rates of greater than 95 % [15–21]. Intermediate-risk disease is treated with surgery and chemotherapy with survival rates of greater than 90 % [15, 16, 22–24]. In contrast, high-risk disease is treated with intensive multimodality therapy (including high-dose chemotherapy, radiation therapy, and stem cell transplantation) with long-term survival rates of approximately 30–40 % [15, 16, 25, 26].

Multiple clinical and imaging tests are used in neuroblastoma, both at diagnosis and during follow-up, to ensure accurate disease assessment. Clinical testing includes bone marrow biopsy and urine catecholamine levels. Imaging evaluation includes both anatomic and functional imaging modalities [27, 28].

CT and MRI are the anatomic imaging modalities recommended for neuroblastoma. They are used to evaluate the primary tumor and involved lymph nodes, including 3D measurements and assessment of imaging-defined risk factors [4–6, 29–34]. MRI is the preferred anatomic imaging modality for tumors which extend into the spinal canal [33–35].

Iodine-123-MIBG is the recommended first-line functional imaging agent for neuroblastoma, allowing visualization of the primary tumor and metastatic sites. Technetium-99m-MDP bone scans and/or ^{18}F-FDG PET scans are recommended for evaluation of MIBG-negative patients [4–6].

Multiple novel PET radiopharmaceuticals have been investigated for use in neuroblastoma, including ^{11}C-hydroxyephedrine (^{11}C- HED), ^{11}C-epinephrine, ^{18}F-fluorodopamine (F-18 DA), ^{18}F-dihydroxyphenylalanine (^{18}F-DOPA), ^{18}F-fluorothymidine (^{18}F-FLT),

^{68}Ga-DOTA-Tyr3-octreotide (^{68}Ga-DOTATOC), ^{18}F-fluoro-3-iodobenzylguanidine (FIBG), and P-^{18}F-fluorobenzylguanidine (PFBG) [36–50]. However, regulatory issues and the PET chemistry expertise needed for synthesis limit availability of these novel radiopharmaceuticals, making it unlikely that they will have a major role in neuroblastoma imaging in the near future. The remainder of this chapter will discuss ^{123}I-MIBG, ^{99m}Tc-MDP, and ^{18}F-FDG imaging of neuroblastoma.

Metaiodobenzylguanidine (MIBG) Scintigraphy

MIBG is related to norepinephrine, entering neural crest cells via the type I catecholamine reuptake system with concentration in the cell cytoplasm. MIBG is highly specific for neuroendocrine tumors, such as neuroblastoma and pheochromocytoma [51–55].

Iodine-131-MIBG was initially used for neuroblastoma imaging [56, 57], as ^{123}I-MIBG was not FDA approved in the USA until 2008. However, ^{123}I-MIBG is now commercially available and preferred for diagnostic imaging as it gives superior image quality at a lower patient radiation dose [58]. Administered doses of ^{131}I-MIBG are limited by its relatively long physical half-life (8 days), high-energy photon (364 keV), and beta particle emission. In contrast, ^{123}I-MIBG has a shorter physical half-life (13 h) and an ideal photon energy for gamma camera and SPECT imaging (159 keV), without beta particle emission.

Patient Preparation

Thyroid uptake of free iodide should be blocked by administration of saturated solution of potassium iodide (SSKI). The dosage and timing of SSKI administration vary with local practice. Although a single SSKI dose at the time of MIBG injection has been shown to adequately block thyroid uptake [59], many sites will administer SSKI doses for 2–3 days starting on the day before ^{123}I-MIBG administration [60–62].

Numerous medications interfere with MIBG uptake, with potential to affect the results of MIBG imaging. Some of these medications (such as phenylephrine, tricyclic antidepressants, and labetalol) are used in children. Medications should therefore be reviewed when scheduling MIBG imaging. Any interfering medications should be discussed with the referring physician with discontinuation for an appropriate time frame when possible [60].

Imaging Technique

The North American Consensus Guidelines recommend an ^{123}I-MIBG administered activity of 0.14 mCi/kg (5.2 MBq/kg) with a minimum dose of 1 mCi (37 MBq) and a maximum dose of 10 mCi (370 MBq); alternatively the European Association of Nuclear Medicine dosage card may be used for patients weighing more than 10 kg [63].

Planar and SPECT (and/or SPECT/CT) imaging typically is performed 24 h after ^{123}I-MIBG injection. Planar imaging includes anterior and posterior whole-body images, which can be performed as overlapping spot images or as a whole-body acquisition. Whole-body planar images are frequently supplemented with lateral views of the skull. Additional planar images can be performed at 48 h if needed to clarify uptake abnormalities or allow clearance of bowel activity [60–62].

SPECT generally includes the abdomen or the primary tumor site if it lies outside of the abdomen. SPECT often improves diagnostic accuracy and certainty of lesion detection, especially for small lesions or lesions near sites of physiologic uptake. SPECT also improves anatomic localization and facilitates correlation with CT and MRI [64–66]. SPECT images can be co-registered and fused to separately acquired CT and MRI studies if patient positioning is similar.

Integrated SPECT/CT (with imaging performed on the same gantry) has more recently become an important diagnostic tool in oncology patients. In comparison to SPECT alone, SPECT/CT further improves MIBG uptake localization and certainty of lesion detection [67–70].

Medium-energy collimators are preferred over low-energy high-resolution collimators for both

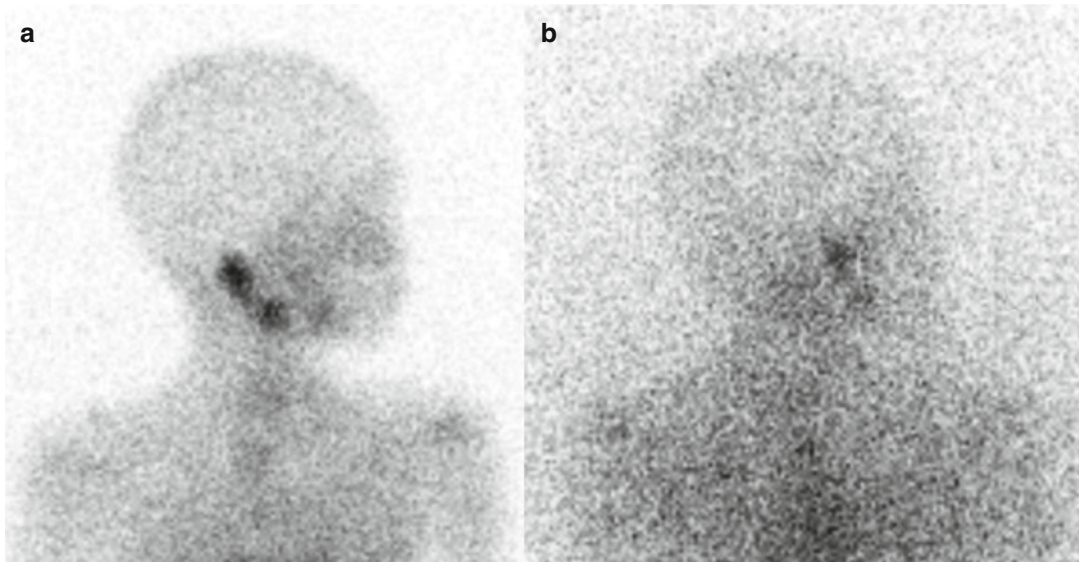

Fig. 19.1 Lateral planar ^{123}I-MIBG images of the skull obtained with (**a**) medium-energy and (**b**) low-energy high-resolution collimators. Use of medium-energy collimation gives higher image quality. Differences in image quality occur at all body masses but become more apparent as patient size increases

planar and SPECT acquisition. Approximately 3 % of photons emitted by ^{123}I-MIBG have energies above 400 keV. Medium-energy collimators significantly reduce septal penetration from these high-energy photons, improving image quality (Fig. 19.1) [71]. Sedation is required for children who are unable to remain still during planar and SPECT imaging. Toilet-trained patients should be encouraged to void prior to imaging.

Clinical Applications

Iodine-123-MIBG imaging is recommended to evaluate neuroblastoma at diagnosis and to monitor MIBG-avid disease during and after therapy (Figs. 19.2 and 19.3) [4–6, 62]. Iodine-123-MIBG imaging also is necessary to determine eligibility for ^{131}I-MIBG therapy, as documentation of MIBG-avid disease is needed prior to treatment. The International Neuroblastoma Risk Group Task Force recently developed guidelines for the evaluation of disease extent by ^{123}I-MIBG scans [62].

Iodine-123-MIBG has a sensitivity of 88–93 % and a specificity of 83–92 % in neuroblastoma [64]. More than 90 % of neuroblastomas will demonstrate MIBG uptake, allowing visualization of both the primary tumor and metastatic sites. At diagnosis, ^{123}I-MIBG imaging is a sensitive whole-body method to evaluate both soft tissue and cortical bone/bone marrow disease. It is therefore an essential tool for initial staging [62].

During therapy, ^{123}I-MIBG imaging is useful for assessing disease response. At the primary tumor site, MIBG imaging differentiates residual active tumor from post-therapy changes which may be seen on CT or MR [62]. MIBG imaging depicts response of cortical bone metastases to therapy, while bone scan and CT may give false-positive results due to continued bone healing in the absence of tumor [27, 72]. MIBG imaging also depicts response of bone marrow metastases to therapy, while interpretation of MRI and ^{18}F-FDG PET scans may be complicated by post-therapy bone marrow changes [73–76].

During surveillance, ^{123}I-MIBG has been shown to be highly sensitive for relapsed bone metastases, with a detection rate of 94 % (compared to 43 % for ^{18}F-FDG PET) [62, 77]. Iodine-123-MIBG imaging also has been shown

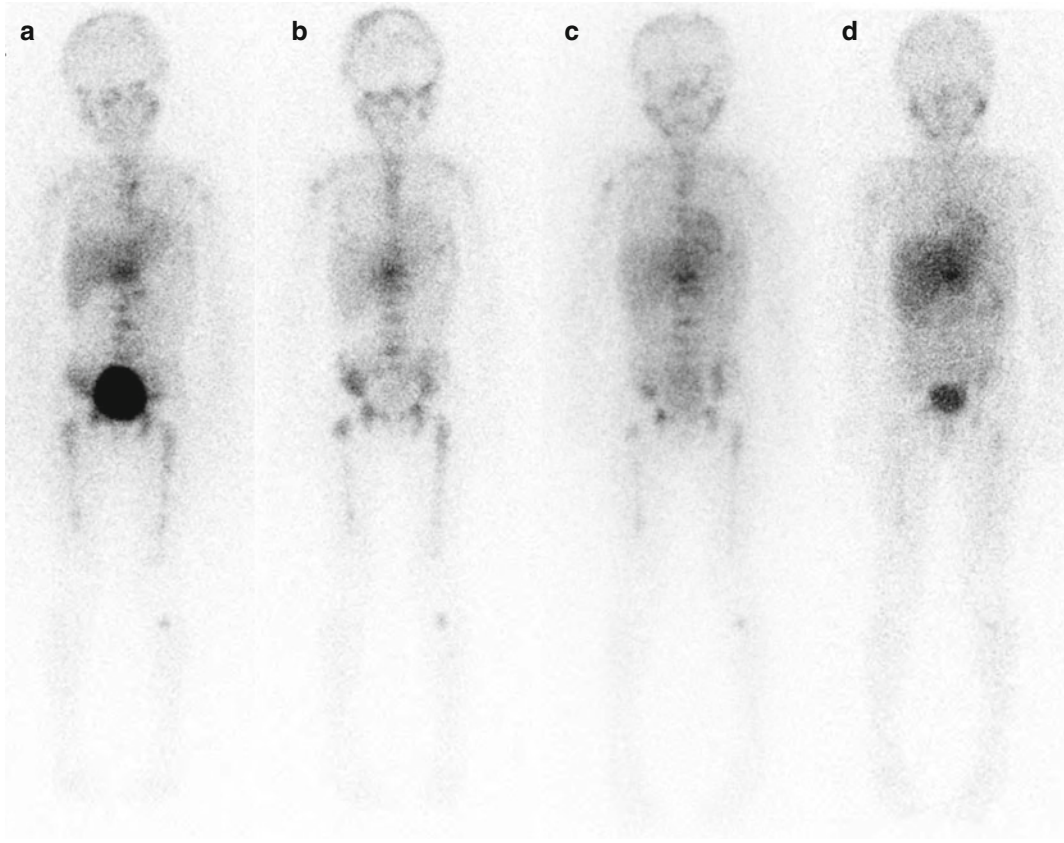

Fig. 19.2 Serial anterior planar ^{123}I-MIBG images obtained in a stage 4 patient. (**a**) At diagnosis, uptake is seen in the midline upper abdominal primary tumor and extensive metastases throughout the appendicular and axial skeleton, including the skull. (**b**) At 6 weeks and (**c**) at 6 months, persistent uptake is seen in both the primary tumor and diffuse skeletal metastases. (**d**) At 12 months, some improvement is seen in skeletal metastatic disease

to be a sensitive method to evaluate for unsuspected disease relapse, with a detection rate of 82 % (compared to 36 % for bone scan and 34 % for bone marrow biopsy) [78].

The results of ^{123}I-MIBG imaging can have prognostic implications. At diagnosis, the extent of MIBG-avid disease may predict response to chemotherapy in children over 1 year of age who have metastatic disease [79]. After initial chemotherapy, persistence of ^{123}I-MIBG uptake in cortical bone and bone marrow may be associated with poor prognosis [80–82]. During surveillance, high-risk patients with unsuspected relapses detected by ^{123}I-MIBG may have longer survival times than high-risk patients with symptomatic relapses [78].

Semiquantitative scoring systems have been described for MIBG imaging of neuroblastoma, with scores correlating with response and survival in some but not all studies [79, 83–89]. Although not yet widely used in clinical practice, scoring systems have been used in research trials to improve interobserver agreement and precision of reporting. Scoring systems divide the skeleton into 6–12 compartments, with each compartment scored for disease extent. The individual compartment scores are added together to give a cumulative score. The Children's Oncology Group (COG) and the New Approaches to Neuroblastoma Therapy (NANT) consortium use the Curie scoring system (Fig. 19.4) [62, 83].

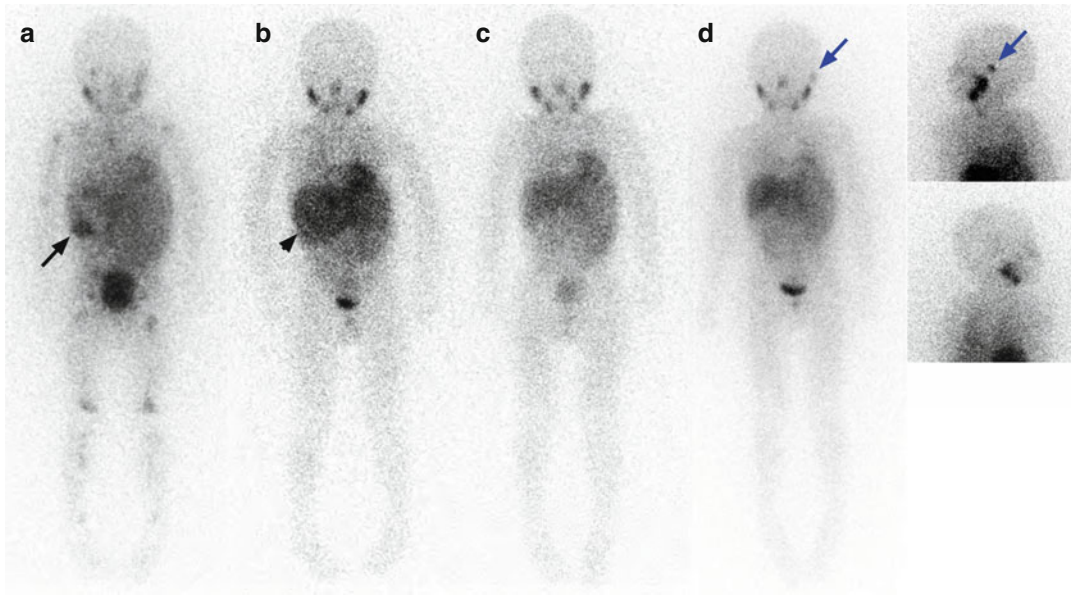

Fig. 19.3 Serial anterior planar ^{123}I-MIBG images obtained in a stage 4 patient. (**a**) At diagnosis, uptake is seen in the right upper quadrant primary tumor (*black arrow*) and scattered skeletal metastases. (**b**) At 1 month, no abnormal skeletal uptake is seen with only minimal residual uptake at the primary tumor site (*black arrowhead*), better demonstrated on SPECT imaging (not shown). (**c**) At 6 months, ^{123}I-MIBG images have normalized. (**d**) At 18 months, an unsuspected recurrence is seen in the left temporal bone (*blue arrows*)

Potential Pitfalls

False-Positive Studies

Physiologic MIBG uptake is normally seen in the salivary glands, olfactory mucosa, myocardium, liver, and bowel. Physiologic adrenal gland activity also may be demonstrated, especially after contralateral adrenalectomy. Urinary excretion of ^{123}I-MIBG results in physiologic accumulation in the kidneys and bladder. Low-level uptake also may be seen in the lungs on 24-h images [90, 91]. More focal lung uptake has been described in areas of atelectasis and pneumonia, but this is rarely seen [92, 93]. Physiologic uptake of ^{123}I-MIBG in brown adipose tissue is, most often seen in the neck and supraclavicular regions [94, 95].

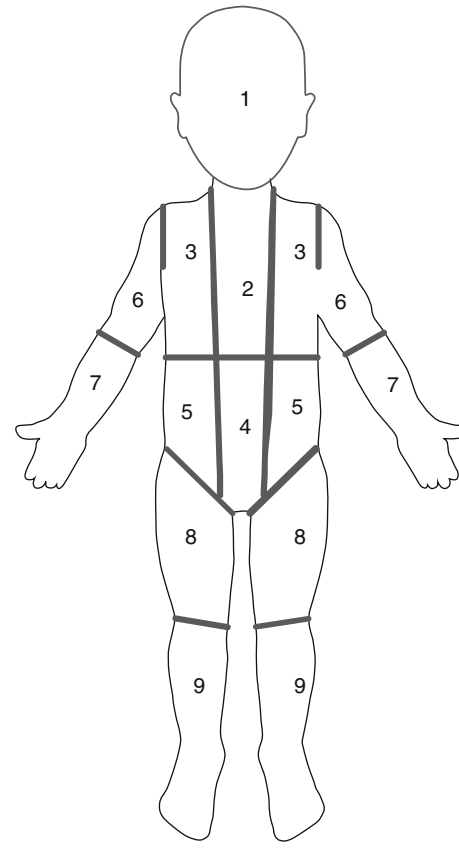

Fig. 19.4 The Curie scoring system divides the skeleton into nine compartments with a tenth compartment used for soft tissue disease. Each compartment is scored for disease extent, where *0* no disease sites, *1* one disease site, *2* more than one disease site (<50 % involvement), and *3* diffuse disease (>50 % involvement). Compartment scores are added together to give a cumulative score

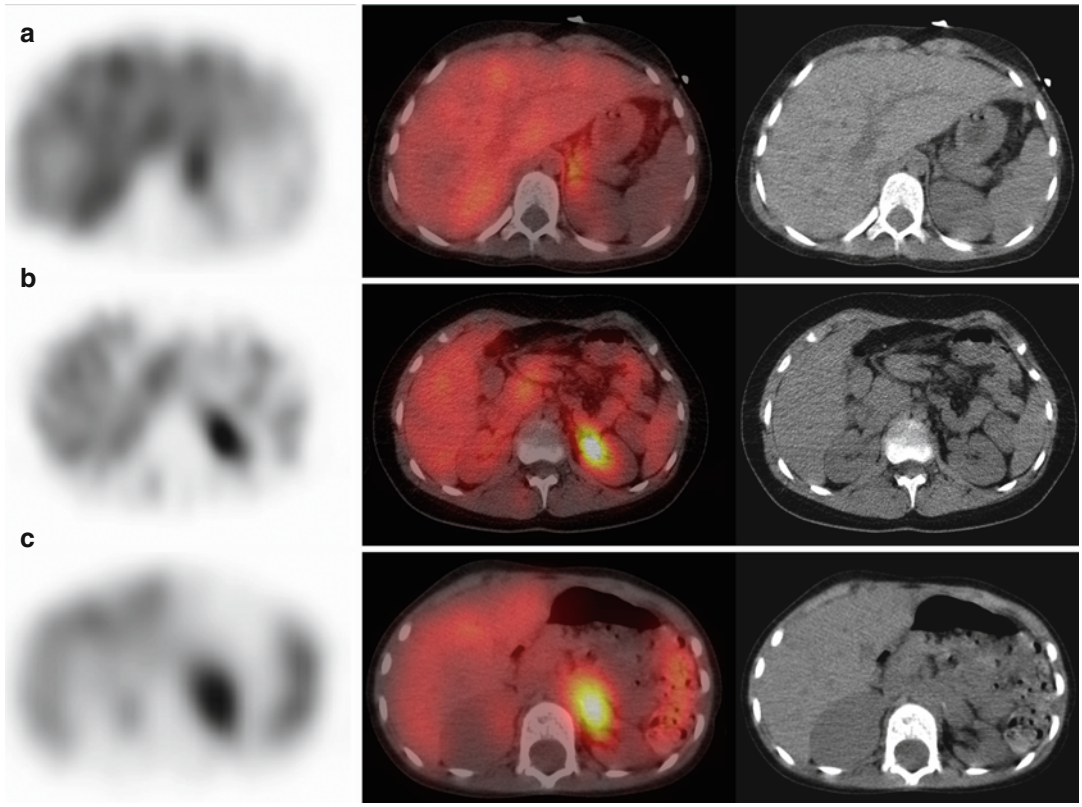

Fig. 19.5 Iodine-123-MIBG SPECT/CT images in three different patients with focal uptake in the left retroperitoneum. (**a**) Physiologic uptake in the normal left adrenal gland. (**b**) Physiologic accumuation in the left renal pelvis reflects urinary excretion of tracer. (**c**) Abnormal uptake in a residual left retroperitoneal soft tissue mass in the region of the renal vessels represents neuroblastoma; the left kidney is noted to be atrophic with compensatory hypertrophy of the right kidney

Misinterpretation of physiologic foci of uptake can result in false-positive MIBG studies [64, 96, 97]. Alternatively, areas of physiologic uptake can obscure small areas of tumor uptake [28]. SPECT and SPECT/CT can improve diagnostic accuracy in areas where physiologic uptake and tumor are both common, especially the retroperitoneum and upper abdomen (Fig. 19.5) [64–70].

The right and left hepatic lobes normally demonstrate significant differences in uptake, with relatively higher uptake in the left hepatic lobe [98]. Physiologic ^{123}I-MIBG uptake in the liver is often heterogeneous, especially on SPECT images. Liver uptake must therefore be interpreted with caution to avoid false-positive studies [66]. Hepatic metastases can be demonstrated with ^{123}I-MIBG, although small metastases may be difficult to visualize. Correlation with CT or MRI is often helpful when hepatic metastases are suspected (Fig. 19.6).

Iodine-123 MIBG uptake in mature ganglioneuromas or other neuroendocrine tumors can be falsely interpreted as uptake in neuroblastoma [64, 96].

False-Negative Studies

Less than 10 % of neuroblastomas demonstrate no MIBG uptake, resulting in false-negative studies. Some neuroblastomas will be MIBG-negative at diagnosis, while others become MIBG-negative during therapy. Patients can have both MIBG-avid and non-avid disease sites at the same time [99–101].

False-negative MIBG studies are also seen in patients with minimal residual disease after therapy [64]. Iodine-123-MIBG can fail to detect subtle bone marrow involvement, usually when

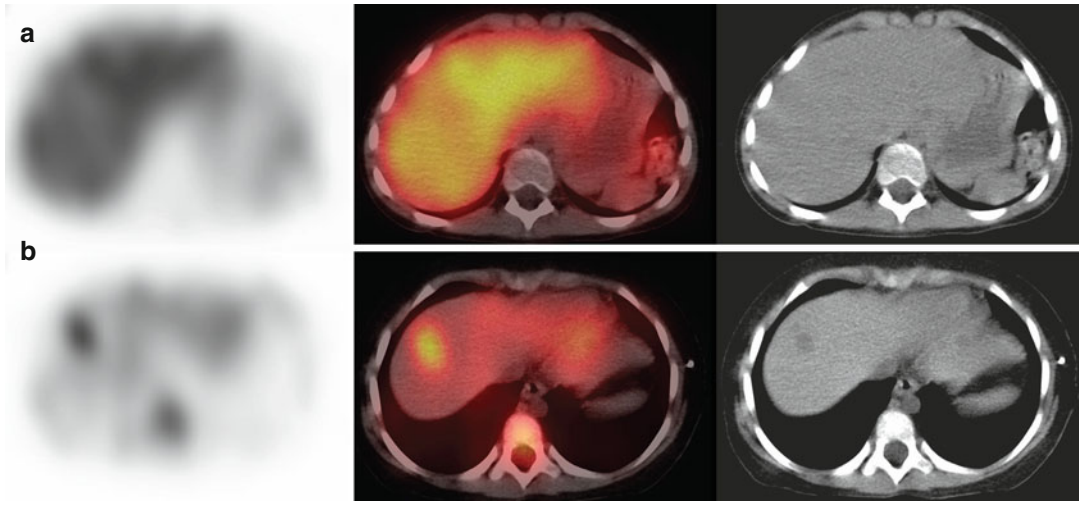

Fig. 19.6 Iodine-123-MIBG SPECT/CT images in two different patients. (**a**) Relatively increased uptake is seen within the left hepatic lobe, a common normal finding. (**b**) Focal increased uptake is seen at the hepatic dome, corresponding to a hypodense liver metastasis

involvement is less than 10 %. Bone marrow biopsy is therefore a standard part of neuroblastoma evaluation [28, 77, 82, 97, 102]. Interestingly, to be classified as a stage 4S or MS, infants must have less than 10 % bone marrow involvement with bone marrow which is ^{123}I-MIBG negative [4, 5].

The sensitivity of disease detection with MIBG increases with increasing administered activities. This is seen when ^{123}I-MIBG pre-therapy diagnostic scans are compared with immediate post-therapy ^{131}I-MIBG scans, which often demonstrate more disease sites [62, 70, 103, 104].

^{99m}Tc-Methylene Diphosphonate (^{99m}Tc-MDP) Bone Scan

Technetium-99m-MDP is taken up primarily in the mineral phase of bone, with relatively increased uptake at sites of bone formation and increased blood flow. Uptake abnormalities are demonstrated at sites of trauma, infection/inflammation, and benign or malignant bony lesions. Technetium-99m-MDP is therefore less specific for neuroblastoma than ^{123}I-MIBG, which utilizes the type I catecholamine reuptake system for uptake into neural crest cells.

Imaging Technique

The North American Consensus Guidelines recommend a ^{99m}Tc-MDP administered activity of 0.25 mCi/kg (9.3 MBq/kg) with a minimum dose of 1 mCi (37 MBq); alternatively, the European Association of Nuclear Medicine dosage card may be used [63].

Planar imaging is typically performed 2–4 h after ^{99m}Tc-MDP injection. Planar imaging includes anterior and posterior whole-body images, which can be performed as overlapping spot images or as a whole-body acquisition. Whole-body planar images are frequently supplemented with lateral views of the skull, oblique views of the torso, or lateral views of the extremities if needed to clarify uptake abnormalities. Sedation is required for children who are unable to remain still during planar imaging. Toilet-trained patients should be encouraged to void prior to imaging.

Clinical Applications

In patients with neuroblastoma, ^{99m}Tc-MDP bone scans traditionally have been used to assess for cortical bone metastases. Bone scans also can demonstrate uptake in the primary tumor, partic-

ularly in areas of calcification. In contrast to MIBG scans, bone scans do not demonstrate bone marrow metastases unless they are large enough to affect adjacent cortical bone.

A bone scan often is performed at diagnosis, as studies have shown discrepancies between MIBG and bone scans that can affect staging [81, 105, 106]. However, neuroblastoma patients usually are followed with MIBG scans alone, as bone scans provide little or no additional information during follow-up of patients with MIBG-avid disease [102, 107, 108]. Bone scans are recommended for assessment of patients with MIBG-negative tumors [4–6].

Potential Pitfalls

Physiologic ^{99m}Tc-MDP bone uptake can complicate detection of metastatic disease. Intense physiologic uptake at the growth plates can be problematic, making metaphyseal metastases difficult to visualize. Neuroblastoma often symmetrically involves the long bones, so abnormalities appear similar on side-to-side comparison (Fig. 19.7). False-positive bone scans can be seen after trauma. During and after therapy, persistent uptake at sites of prior metastases can also be seen in the absence of tumor [27, 72].

^{18}F-Fluorodeoxyglucose (FDG) PET and PET/CT

FDG is a glucose analog that is concentrated in metabolically active sites, including most tumors and areas of infection/inflammation. Fluorine-18-FDG is therefore less specific for neuroblastoma than ^{123}I-MIBG, which utilizes the type I catecholamine reuptake system for uptake into neural crest cells.

Patient Preparation

Appropriate patient preparation is important before ^{18}F-FDG PET or PET/CT (see Chap. 3). Patients should be warmed for 30–60 min prior to ^{18}F-FDG administration to limit uptake in brown adipose tissue, with premedication also used at some centers [109–113]. Patients should fast for 4 h prior to ^{18}F-FDG injection. Any glucose-containing intravenous fluids should be discontinued 4 h prior to ^{18}F-FDG administration [114]. After administration, patients should limit physical activity to avoid muscular uptake of ^{18}F-FDG [114].

Imaging Technique

The North American Consensus Guidelines recommend an ^{18}F-FDG administered activity of 0.10–0.14 mCi/kg (3.7–5.2 MBq/kg) with a minimum dose of 1.0 mCi (37 MBq); alternatively, the European Association of Nuclear Medicine dosage card may be used [63]. Appropriate pediatric CT settings should be utilized to minimize radiation dose. PET or PET/CT is performed approximately 1 h after ^{18}F-FDG injection. The lower extremities and skull should routinely be included in the scan, as disease involvement commonly occurs in these areas. Sedation is required for children who are unable to remain still during PET and PET/CT imaging. Toilet-trained patients should be encouraged to void prior to imaging.

Clinical Applications

The majority of neuroblastomas concentrate ^{18}F-FDG both before and after therapy, with uptake seen in both soft tissue and skeletal disease sites [28, 97, 115]. Findings on ^{18}F-FDG scans have been shown to correlate with disease status with serial scans accurately depicting treatment effects and disease evolution [28].

However, when compared to ^{123}I-MIBG, ^{18}F-FDG is often inferior for neuroblastoma evaluation. Fluorine-18-FDG can show lower tumor to non-tumor uptake ratios, especially after therapy [115]. Fluorine-18-FDG PET is less sensitive for neuroblastoma detection, especially in high-risk or relapsed disease. The inferiority of ^{18}F-FDG PET often is due to poorer depiction of cortical bone/bone marrow metastases, especially during therapy [76, 77, 116].

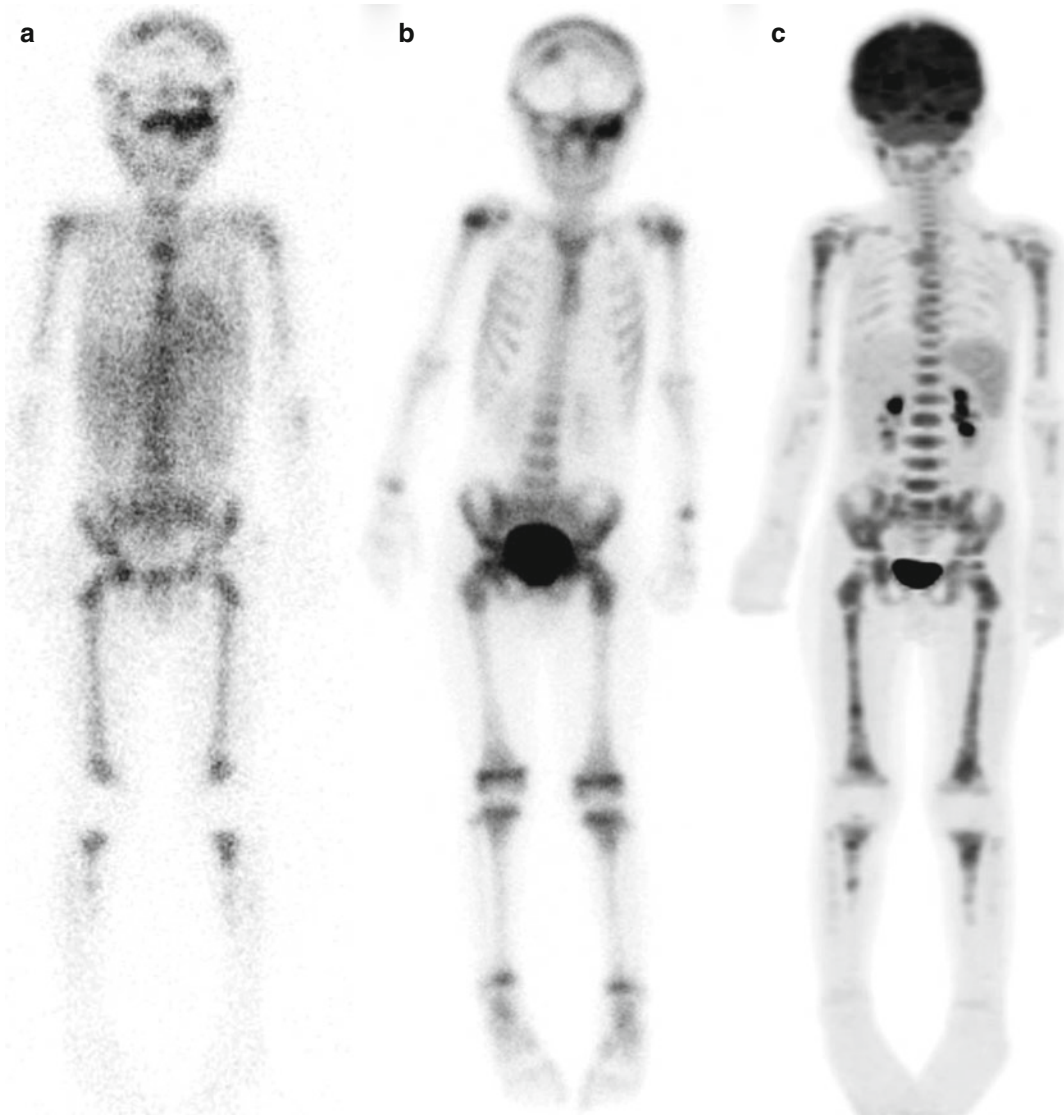

Fig. 19.7 Stage 4 patient imaged at diagnosis. (**a**) Iodine-123-MIBG anterior planar image shows diffuse metastatic disease throughout the axial and appendicular skeleton, including the skull. (**b**) Technetium-99m-MDP anterior planar image shows multiple bony metastases in the skull, pelvis, and long bones; however, extent of involvement in the spine and long bones is somewhat difficult to judge given the physiologic uptake in bone and diffuse symmetric disease involvement. (**c**) Fluorine-18-FDG PET MIP shows diffuse metastatic disease throughout the axial and appendicular skeleton; extent of skull involvement is difficult to visualize due to adjacent brain activity, although the larger skull lesions can be visualized on tomographic images (see Fig. 19.10)

Fluorine-18-FDG PET is most useful for imaging neuroblastomas that fail to or weakly accumulate ^{123}I-MIBG [76, 97, 115, 116] and is recommended as an option for evaluation of MIBG-negative tumors (Fig. 19.8) [5, 6]. Use of ^{18}F-FDG PET should be considered when CT/MR or clinical findings suggest more disease than demonstrated by ^{123}I-MIBG scans [97, 116–118]. A study of patients with MIBG-negative tumors or discrepancies between their ^{123}I-MIBG scans and CT/MRI or clinical findings showed that ^{18}F-FDG PET was more sensitive (78 %

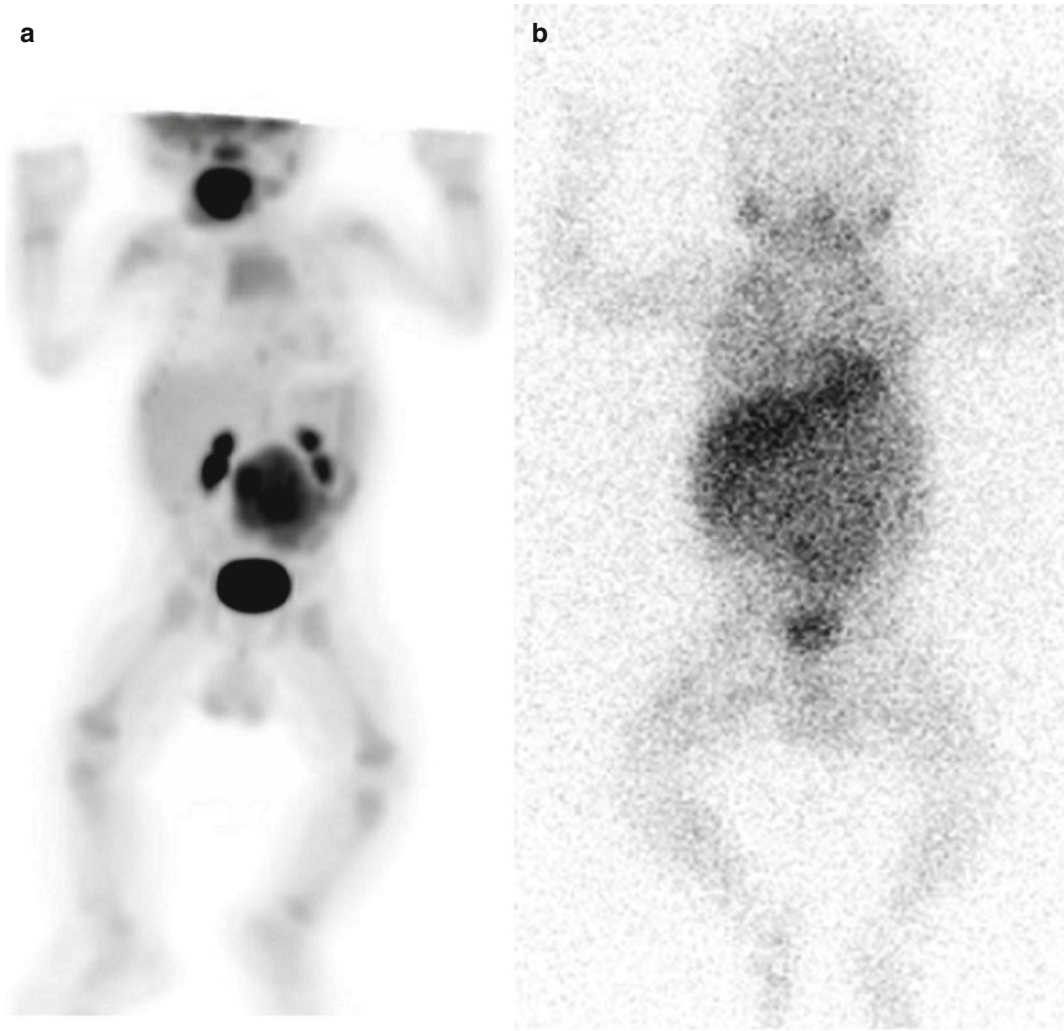

Fig. 19.8 Stage 3 patient imaged at diagnosis (**a**). FDG anterior projection MIP image demonstrates marked uptake in the large abdominal primary tumor; mild diffuse physiologic uptake in the bone marrow is also noted. (**b**) Iodine-123-MIBG anterior planar image demonstrates minimal uptake in the large abdominal primary tumor, slightly above background (This figure/research was originally published in *JNM*. Sharp et al. [76] © by the Society of Nuclear Medicine and Molecular Imaging, Inc., with permission)

versus 50 %) and specific (92 % versus 75 %) than ^{123}I-MIBG in this population, although review of both ^{123}I-MIBG scan and ^{18}F-FDG PET together gave the highest sensitivity (85 %) [97].

Fluorine-18-FDG PET and ^{123}I-MIBG scans can be complimentary, with each study sometimes demonstrating disease sites not identified with the other [28, 76, 97, 115]. Concurrent ^{123}I-MIBG scans and ^{18}F-FDG PET or PET/CT may therefore be useful to evaluate the full extent of disease involvement, especially at therapeutic decision points [76].

The intrinsic tomographic nature and higher spatial resolution of ^{18}F-FDG PET and PET/CT improves disease localization and detection of small lesion [28, 77]. Fluorine-18-FDG PET can be useful especially for identifying disease sites in the chest, abdomen, and pelvis [76].

A study including 10 patients with stage 1 and 2 neuroblastoma suggested that ^{18}F-FDG PET

may be superior to ^{123}I-MIBG in this population. In this study, 6 patients had better depiction of their primary tumor and/or regional metastases with ^{18}F-FDG PET [76]. A study including 17 soft tissue lesions suggested that ^{18}F-FDG PET may have higher sensitivity than ^{123}I-MIBG scans for soft tissue lesions. In this study, 6 lesions were seen only on ^{18}F-FDG PET [77]. However, larger studies are needed to confirm these findings.

A study reviewing neuroblastoma staging evaluations (including ^{18}F-FDG PET, ^{123}I-MIBG, ^{99m}Tc-MDP bone scans, CT/MRI, urine catecholamines, and bone marrow biopsy) suggested that ^{18}F-FDG PET and bone marrow sampling may be sufficient to monitor for progressive disease after tumor resection, as long as there were no skull lesions [28]. However, ^{123}I-MIBG remains a standard part of neuroblastoma assessment with a later study from this institution stating that ^{123}I-MIBG is essential for valid estimation of relapse-free survival in high-risk neuroblastoma patients [78].

Potential Pitfalls

Fluorine-18-FDG is a less-specific imaging agent than ^{123}I-MIBG. Physiologic uptake and uptake at sites of inflammation/infection can complicate image interpretation [28, 115]. Benign fibro-osseous lesions can also demonstrate variable ^{18}F-FDG uptake and mimic cortical bone metastases [119, 120].

Assessment of bone marrow involvement can be especially problematic. Physiologic ^{18}F-FDG uptake in bone marrow is seen in the absence of tumor [77, 115, 116]. Bone marrow metastases also sometimes produce ^{18}F-FDG uptake patterns that are indistinguishable from normal or physio-

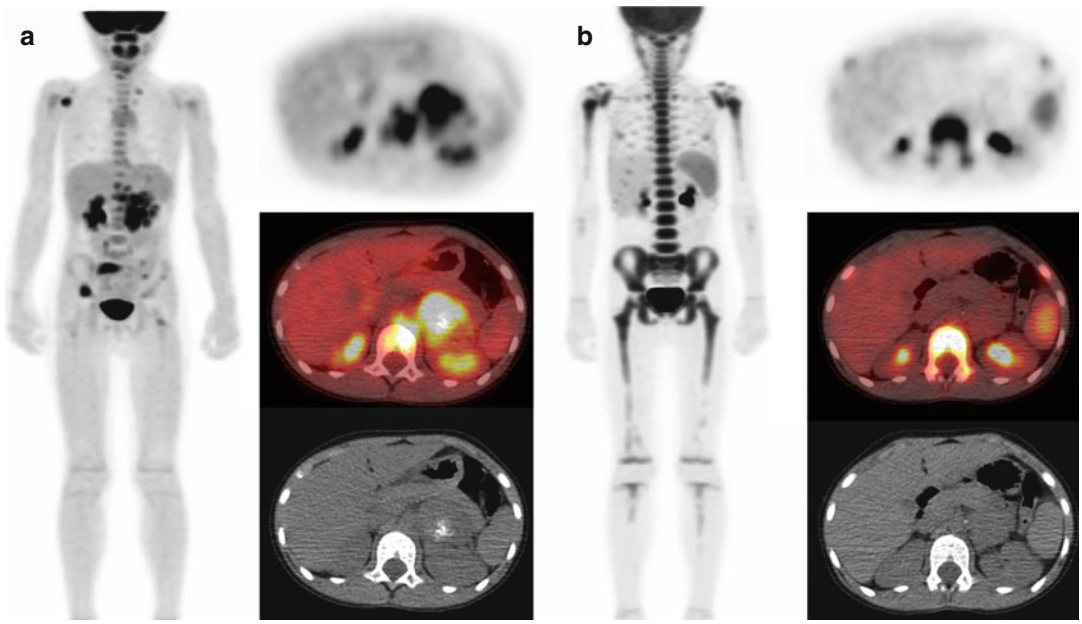

Fig. 19.9 Serial ^{18}F-FDG anterior projection MIP and axial PET/CT images in a patient with stage 4 neuroblastoma. (**a**) At diagnosis, ^{18}F-FDG uptake is seen in the primary partially calcified left retroperitoneal tumor, retroperitoneal lymphadenopathy, and multiple skeletal metastases (most notably involving the right glenoid, L1 vertebral body, right sacrum, and right iliac bone). (**b**) After chemotherapy and G-CSF therapy, intense diffuse bone marrow uptake is seen, potentially obscuring or mimicking metastatic disease; the primary left retroperitoneal tumor has decreased in size and no longer demonstrates FDG avidity (This figure/research was originally published in *JNM*. Sharp et al. [76] © by the Society of Nuclear Medicine and Molecular Imaging, Inc., with permission)

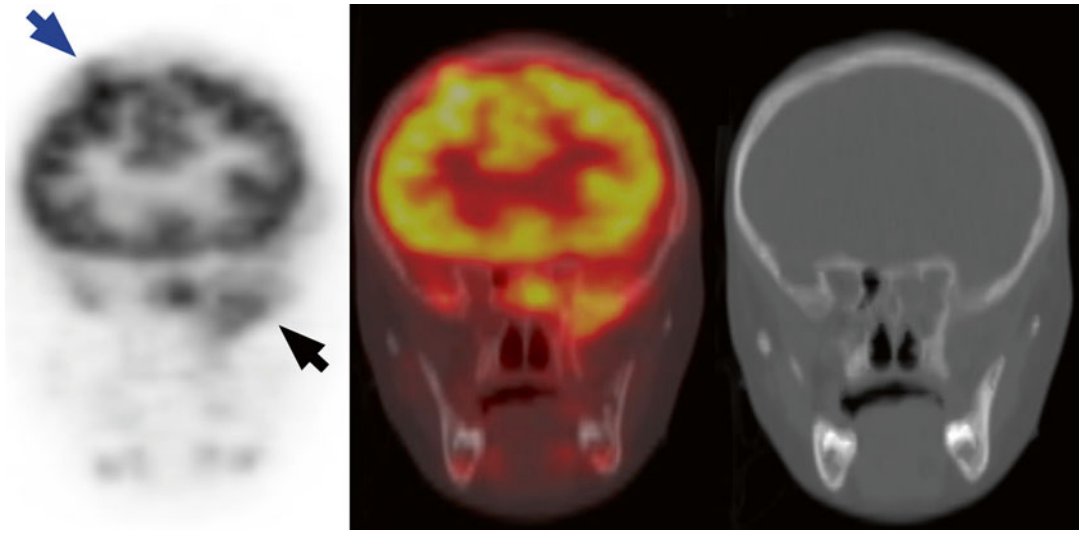

Fig. 19.10 Patient with stage 4 neuroblastoma also shown in Fig. 19.7. Coronal ^{18}F-FDG PET/CT images show abnormal uptake within the large right frontal (*blue arrow*) and left skull base (*black arrow*) lesions. Other smaller skull lesions are not as well seen

logic bone marrow activity [76]. During or after granulocyte colony-stimulating factor (G-CSF) therapy, extensive ^{18}F-FDG uptake in bone marrow can obscure or mimic metastatic disease [76, 77, 116] (Fig. 19.9). Like ^{123}I-MIBG, ^{18}F-FDG also can fail to detect minimal bone marrow disease [28, 77]. For example, cranial vault lesions can be difficult to identify near adjacent brain activity [28, 77, 115, 116], although large skull lesions usually can be identified (Figs. 19.7 and 19.10).

^{131}I-MIBG Therapy

Targeted therapy for neuroblastoma utilizing ^{131}I-MIBG is made possible by the radiosensitivity and MIBG avidity of most tumors. Clinical studies have evaluated the use of ^{131}I-MIBG in neuroblastoma therapy, both as a single agent and in combination with other agents including radiation sensitizers and cytotoxic chemotherapy [121]. Initial studies focused on use in patients with refractory or recurrent neuroblastoma, with objective responses seen in a significant minority of patients. More recent studies have investigated the use of ^{131}I-MIBG therapy in newly diagnosed high risk patients. In North America, ^{131}I-MIBG therapy currently is administered as an investigational agent at several sites in the United States and Canada. Myelosuppression is the main toxicity of ^{131}I-MIBG therapy. The maximum administered dose may depend upon the availability of autologous stem cells that can be used for bone marrow rescue.

References

1. Lonergan GJ, Schwab CM, Suarez ES, et al. Neuroblastoma, ganglioneuroblastoma, and ganglioneuroma: radiologic-pathologic correlation. Radiographics. 2002;22(4):911–34.
2. Kaatsch P. Epidemiology of childhood cancer. Cancer Treat Rev. 2010;36(4):277–85.
3. DuBois SG, Kalika Y, Lukens JN, et al. Metastatic sites in stage IV and IVS neuroblastoma correlate with age, tumor biology, and survival. J Pediatr Hematol Oncol. 1999;21(3):181–9.
4. Brodeur GM, Pritchard J, Berthold F, et al. Revisions of the international criteria for neuroblastoma diagnosis, staging, and response to treatment. J Clin Oncol. 1993;11(8):1466–77.
5. Monclair T, Brodeur GM, Ambros PF, et al. The International Neuroblastoma Risk Group (INRG) staging system: an INRG task force report. J Clin Oncol. 2009;27(2):298–303.
6. Brisse HJ, McCarville MB, Granata C, et al. Guidelines for imaging and staging of neuroblas-

tic tumors: consensus report from the International Neuroblastoma Risk Group Project. Radiology. 2011;261(1):243–57.
7. Gunther P, Holland-Cunz S, Schupp CJ, et al. Significance of image-defined risk factors for surgical complications in patients with abdominal neuroblastoma. Eur J Pediatr Surg. 2011;21(5):314–7.
8. Cohn SL, Pearson AD, London WB, et al. The International Neuroblastoma Risk Group (INRG) classification system: an INRG Task Force report. J Clin Oncol. 2009;27(2):289–97.
9. Moroz V, Machin D, Faldum A, et al. Changes over three decades in outcome and the prognostic influence of age-at-diagnosis in young patients with neuroblastoma: a report from the International Neuroblastoma Risk Group Project. Eur J Cancer. 2011;47(4):561–71.
10. London WB, Castleberry RP, Matthay KK, et al. Evidence for an age cutoff greater than 365 days for neuroblastoma risk group stratification in the Children's Oncology Group. J Clin Oncol. 2005;23(27):6459–65.
11. George RE, London WB, Cohn SL, et al. Hyperdiploidy plus nonamplified MYCN confers a favorable prognosis in children 12 to 18 months old with disseminated neuroblastoma: a Pediatric Oncology Group study. J Clin Oncol. 2005;23(27):6466–73.
12. Schmidt ML, Lal A, Seeger RC, et al. Favorable prognosis for patients 12 to 18 months of age with stage 4 nonamplified MYCN neuroblastoma: a Children's Cancer Group study. J Clin Oncol. 2005;23(27):6474–80.
13. Maris JM, Hogarty MD, Bagatell R, et al. Neuroblastoma. Lancet. 2007;369(9579):2106–20.
14. Brodeur GM. Neuroblastoma: biological insights into a clinical enigma. Nat Rev Cancer. 2003;3(3):203–16.
15. Park JR, Eggert A, Caron H. Neuroblastoma: biology, prognosis, and treatment. Hematol Oncol Clin North Am. 2010;24(1):65–86.
16. Maris JM. Recent advances in neuroblastoma. N Engl J Med. 2010;362(23):2202–11.
17. Strother DR, London WB, Schmidt ML, et al. Outcome after surgery alone or with restricted use of chemotherapy for patients with low-risk neuroblastoma: results of Children's Oncology Group study P9641. J Clin Oncol. 2012;30(15):1842–8.
18. Hero B, Simon T, Spitz R, et al. Localized infant neuroblastomas often show spontaneous regression: results of the prospective trials NB95-S and NB97. J Clin Oncol. 2008;26(9):1504–10.
19. Simon T, Spitz R, Faldum A, et al. New definition of low-risk neuroblastoma using stage, age, and 1p and MYCN status. J Pediatr Hematol Oncol. 2004;26(12):791–6.
20. Perez CA, Matthay KK, Atkinson JB, et al. Biologic variables in the outcome of stages I and II neuroblastoma treated with surgery as primary therapy: a Children's Cancer Group study. J Clin Oncol. 2000;18(1):18–26.
21. Nickerson HJ, Matthay KK, Seeger RC, et al. Favorable biology and outcome of stage IV-S neuroblastoma with supportive care or minimal therapy: a Children's Cancer Group study. J Clin Oncol. 2000;18(3):477–86.
22. Matthay KK, Perez C, Seeger RC, et al. Successful treatment of stage III neuroblastoma based on prospective biologic staging: a Children's Cancer Group study. J Clin Oncol. 1998;16(4):1256–64.
23. Schmidt ML, Lukens JN, Seeger RC, et al. Biologic factors determine prognosis in infants with stage IV neuroblastoma: a prospective Children's Cancer Group study. J Clin Oncol. 2000;18(6):1260–8.
24. Baker DL, Schmidt ML, Cohn SL, et al. Outcome after reduced chemotherapy for intermediate-risk neuroblastoma. N Engl J Med. 2010;363(14):1313–23.
25. Matthay KK, Villablanca JG, Seeger RC, et al. Treatment of high-risk neuroblastoma with intensive chemotherapy, radiotherapy, autologous bone marrow transplantation, and 13-cis-retinoic acid. Children's Cancer Group. N Engl J Med. 1999;341(16):1165–73.
26. Matthay KK, Reynolds CP, Seeger RC, et al. Long-term results for children with high-risk neuroblastoma treated on a randomized trial of myeloablative therapy followed by 13-cis-retinoic acid: a Children's Oncology Group study. J Clin Oncol. 2009;27(7):1007–13.
27. Kushner BH. Neuroblastoma: a disease requiring a multitude of imaging studies. J Nucl Med. 2004;45(7):1172–88.
28. Kushner BH, Yeung HW, Larson SM, et al. Extending positron emission tomography scan utility to high-risk neuroblastoma: fluorine-18 fluorodeoxyglucose positron emission tomography as sole imaging modality in follow-up of patients. J Clin Oncol. 2001;19(14):3397–405.
29. Stark DD, Moss AA, Brasch RC, et al. Neuroblastoma: diagnostic imaging and staging. Radiology. 1983;148(1):101–5.
30. Stark DD, Brasch RC, Moss AA, et al. Recurrent neuroblastoma: the role of CT and alternate imaging tests. Radiology. 1983;148(1):107–12.
31. Golding SJ, McElwain TJ, Husband JE. The role of computed tomography in the management of children with advanced neuroblastoma. Br J Radiol. 1984;57(680):661–6.
32. Siegel MJ, Ishwaran H, Fletcher BD, et al. Staging of neuroblastoma at imaging: report of the Radiology Diagnostic Oncology Group. Radiology. 2002;223(1):168–75.
33. Hugosson C, Nyman R, Jorulf H, et al. Imaging of abdominal neuroblastoma in children. Acta Radiol. 1999;40(5):534–42.
34. Sofka CM, Semelka RC, Kelekis NL, et al. Magnetic resonance imaging of neuroblastoma using current techniques. Magn Reson Imaging. 1999;17(2):193–8.
35. Slovis TL, Meza MP, Cushing B, et al. Thoracic neuroblastoma: what is the best imaging modality for evaluating extent of disease? Pediatr Radiol. 1997; 27(3):273–5.
36. Ilias I, Shulkin B, Pacak K. New functional imaging modalities for chromaffin tumors, neuroblastomas and ganglioneuromas. Trends Endocrinol Metab. 2005;16(2):66–72.

37. Rufini V, Calcagni ML, Baum RP. Imaging of neuroendocrine tumors. Semin Nucl Med. 2006;36(3):228–47.
38. Chen CC, Carrasquillo JA. Molecular imaging of adrenal neoplasms. J Surg Oncol. 2012;106(5):532–42.
39. Franzius C, Hermann K, Weckesser M, et al. Whole-body PET/CT with 11C-meta-hydroxyephedrine in tumors of the sympathetic nervous system: feasibility study and comparison with 123I-MIBG SPECT/CT. J Nucl Med. 2006;47(10):1635–42.
40. Shulkin BL, Wieland DM, Baro ME, et al. PET hydroxyephedrine imaging of neuroblastoma. J Nucl Med. 1996;37(1):16–21.
41. Shulkin BL, Wieland DM, Castle VP, et al. Carbon-11 epinephrine PET imaging of neuroblastoma. J Nucl Med. 1999;40s:129 [abstract].
42. Lopci E, Piccardo A, Nanni C, et al. 18F-DOPA PET/CT in neuroblastoma: comparison of conventional imaging with CT/MR. Clin Nucl Med. 2012;37(4):e73–8.
43. Piccardo A, Lopci E, Conte M, et al. Comparison of 18F-dopa PET/CT and 123I-MIBG scintigraphy in stage 3 and 4 neuroblastoma: a pilot study. Eur J Nucl Med Mol Imaging. 2012;39(1):57–71.
44. Tzen K, Wang L, Lu M. Characterization of neuroblastic tumors using F-18 DOPA PET. J Nucl Med. 2007;48s:117 [abstract].
45. Valentiner U, Haane C, Peldschus K, et al. [18F]FDG and [18F]FLT PET-CT and MR imaging of human neuroblastoma in a SCID mouse xenograft model. Anticancer Res. 2008;28(5A):2561–8.
46. Krieger-Hinck N, Gustke H, Valentiner U, et al. Visualisation of neuroblastoma growth in a Scid mouse model using [18F]FDG and [18F]FLT-PET. Anticancer Res. 2006;26(5A):3467–72.
47. Kroiss A, Putzer D, Uprimny C, et al. Functional imaging in phaeochromocytoma and neuroblastoma with 68Ga-DOTA-Tyr3-octreotide positron emission tomography and 123I-metaiodobenzylguanidine. Eur J Nucl Med Mol Imaging. 2011;38(5):865–73.
48. Vaidyanathan G, Zhao XG, Strickland DK, et al. No-carrier-added iodine-131-FIBG: evaluation of an MIBG analog. J Nucl Med. 1997;38(2):330–4.
49. Vaidyanathan G, Affleck DJ, Zalutsky MR. Validation of 4-[fluorine-18]fluoro-3-iodobenzylguanidine as a positron-emitting analog of MIBG. J Nucl Med. 1995;36(4):644–50.
50. Vaidyanathan G, Affleck DJ, Zalutsky MR. (4-[18F] fluoro-3-iodobenzyl)guanidine, a potential MIBG analogue for positron emission tomography. J Med Chem. 1994;37(21):3655–62.
51. Leung A, Shapiro B, Hattner R, et al. Specificity of radioiodinated MIBG for neural crest tumors in childhood. J Nucl Med. 1997;38(9):1352–7.
52. Sisson JC, Shulkin BL. Nuclear medicine imaging of pheochromocytoma and neuroblastoma. Q J Nucl Med. 1999;43(3):217–23.
53. Shapiro B, Gross MD. Radiochemistry, biochemistry, and kinetics of 131I-metaiodobenzylguanidine (MIBG) and 123I-MIBG: clinical implications of the use of 123I-MIBG. Med Pediatr Oncol. 1987;15(4):170–7.
54. Smets LA, Loesberg C, Janssen M, et al. Active uptake and extravesicular storage of m-iodobenzylguanidine in human neuroblastoma SK-N-SH cells. Cancer Res. 1989;49(11):2941–4.
55. Smets LA, Janssen M, Metwally E, et al. Extragranular storage of the neuron blocking agent meta-iodobenzylguanidine (MIBG) in human neuroblastoma cells. Biochem Pharmacol. 1990;39(12):1959–64.
56. Treuner J, Feine U, Niethammer D, et al. Scintigraphic imaging of neuroblastoma with 131I-iodobenzylguanidine. Lancet. 1984;1(8372):333–4.
57. Geatti O, Shapiro B, Sisson JC, et al. Iodine-131 metaiodobenzylguanidine scintigraphy for the location of neuroblastoma: preliminary experience in ten cases. J Nucl Med. 1985;26(7):736–42.
58. Gelfand MJ. I-123-MIBG and I-131-MIBG imaging in children with neuroblastoma. J Nucl Med. 1996;37s:35 [abstract].
59. Wood DE, Gilday DL, Kellan J. Stable iodine requirements for thyroid gland blockage of iodinated radiopharmaceuticals. J Can Assoc Radiol. 1974;25(4):295–6.
60. Bombardieri E, Giammarile F, Aktolun C, et al. 131I/123I-metaiodobenzylguanidine (mIBG) scintigraphy: procedure guidelines for tumour imaging. Eur J Nucl Med Mol Imaging. 2010;37(12):2436–46.
61. Olivier P, Colarinha P, Feltich J, et al. Guidelines for radioiodinated MIBG scintigraphy in children. Eur J Nucl Med Mol Imaging. 2003;30(5):B45–50.
62. Matthay KK, Shulkin B, Ladenstein R, et al. Criteria for evaluation of disease extent by (123) I-metaiodobenzylguanidine scans in neuroblastoma: a report for the International Neuroblastoma Risk Group (INRG) Task Force. Br J Cancer. 2010;102(9):1319–26.
63. Gelfand MJ, Parisi MT, Treves ST. Pediatric radiopharmaceutical administered doses: 2010 North American consensus guidelines. J Nucl Med. 2011;52(2):318–22.
64. Vik TA, Pfluger T, Kadota R, et al. (123)I-mIBG scintigraphy in patients with known or suspected neuroblastoma: results for a prospective multicenter trial. Pediatr Blood Cancer. 2009;52(7):784–90.
65. Gelfand MJ, Elgazzar AH, Kriss VM, et al. Iodine-123-MIBG SPECT versus planar imaging in children with neural crest tumors. J Nucl Med. 1994;35(11):1753–7.
66. Rufini V, Fisher GA, Shulkin BL, et al. Iodine-123-MIBG imaging of neuroblastoma: utility of SPECT and delayed imaging. J Nucl Med. 1996;37(9):1464–8.
67. Rozovsky K, Koplewitz BZ, Krausz Y, et al. Added value of SPECT/CT for correlation of MIBG scintigraphy and diagnostic CT in neuroblastoma and pheochromocytoma. Am J Roentgenol. 2008;190(4):1085–90.
68. Bar-Sever Z, Steinmetz A, Ash S, et al. The role of MIBG SPECT/CT in children with neuroblastoma. J Nucl Med. 2008;49s:84 [abstract].

69. Sharp SE, Gelfand MJ. Utility of SPECT/CT imaging in neuroblastoma. J Nucl Med. 2009;50s:52 [abstract].
70. Fukuoka M, Taki J, Mochizuki T, et al. Comparison of diagnostic value of I-123 MIBG and high-dose I-131 MIBG scintigraphy including incremental value of SPECT/CT over planar image in patients with malignant pheochromocytoma/paraganglioma and neuroblastoma. Clin Nucl Med. 2011;36(1):1–7.
71. Snay ER, Treves ST, Fahey FH. Improved quality of pediatric 123I-MIBG images with medium-energy collimators. J Nucl Med Technol. 2011;39(2):100–4.
72. Englaro DD, Gelfand MJ, Harris RE, et al. I-131 MIBG imaging after bone marrow transplantation for neuroblastoma. Radiology. 1992;182(2):515–20.
73. Tanabe M, Takahashi H, Ohnuma N, et al. Evaluation of bone marrow metastasis of neuroblastoma and changes after chemotherapy by MRI. Med Pediatr Oncol. 1993;21(1):54–9.
74. Tanabe M, Ohnuma N, Iwai J, et al. Bone marrow metastasis of neuroblastoma analyzed by MRI and its influence on prognosis. Med Pediatr Oncol. 1995;24(5):292–9.
75. Lebtahi N, Gudinchet F, Nenadov-Beck M, et al. Evaluating bone marrow metastasis of neuroblastoma with iodine-123-MIBG scintigraphy and MRI. J Nucl Med. 1997;38(9):1389–92.
76. Sharp SE, Shulkin BL, Gelfand MJ, et al. 123I-MIBG scintigraphy and 18F-FDG PET in neuroblastoma. J Nucl Med. 2009;50(8):1237–43. http://jnm.snmjournals.org/site/misc/permission.xhtml
77. Taggart DR, Han MM, Quach A, et al. Comparison of iodine-123 metaiodobenzylguanidine (MIBG) scan and [18F]fluorodeoxyglucose positron emission tomography to evaluate response after iodine-131 MIBG therapy for relapsed neuroblastoma. J Clin Oncol. 2009;27(32):5343–9.
78. Kushner BH, Kramer K, Modak S, et al. Sensitivity of surveillance studies for detecting asymptomatic and unsuspected relapse of high-risk neuroblastoma. J Clin Oncol. 2009;27(7):1041–6.
79. Suc A, Lumbroso J, Rubie H, et al. Metastatic neuroblastoma in children older than one year: prognostic significance of the initial metaiodobenzylguanidine scan and proposal for a scoring system. Cancer. 1996;77(4):805–11.
80. Ladenstein R, Philip T, Lasset C, et al. Multivariate analysis of risk factors in stage 4 neuroblastoma patients over the age of one year treated with megatherapy and stem-cell transplantation: a report from the European Bone Marrow Transplant Solid Tumor Registry. J Clin Oncol. 1998;16(3):953–65.
81. Perel Y, Conway J, Kletzel M, et al. Clinical impact and prognostic value of metaiodobenzylguanidine imaging in children with metastatic neuroblastoma. J Pediatr Hematol Oncol. 1999;21(1):13–8.
82. Schmidt M, Simon T, Hero B, et al. The prognostic impact of functional imaging with (123)I-mIBG in patients with stage 4 neuroblastoma >1 year of age on a high-risk treatment protocol: results of the German Neuroblastoma Trial NB97. Eur J Cancer. 2008;44(11):1552–8.
83. Ady N, Zucker JM, Asselain B, et al. A new 123I-MIBG whole body scan scoring method – application to the prediction of the response of metastases to induction chemotherapy in stage IV neuroblastoma. Eur J Cancer. 1995;31A(2):256–61.
84. Frappaz D, Bonneu A, Chauvot P, et al. Metaiodobenzylguanidine assessment of metastatic neuroblastoma: observer dependency and chemosensitivity evaluation. The SFOP Group. Med Pediatr Oncol. 2000;34(4):237–41.
85. Hero B, Hunneman DH, Gahr M, et al. Evaluation of catecholamine metabolites, mIBG scan, and bone marrow cytology as response markers in stage 4 neuroblastoma. Med Pediatr Oncol. 2001;36(1):220–3.
86. Matthay KK, Edeline V, Lumbroso J, et al. Correlation of early metastatic response by 123I-metaiodobenzylguanidine scintigraphy with overall response and event-free survival in stage IV neuroblastoma. J Clin Oncol. 2003;21(13):2486–91.
87. Katzenstein HM, Cohn SL, Shore RM, et al. Scintigraphic response by 123I-metaiodobenzylguanidine scan correlates with event-free survival in high-risk neuroblastoma. J Clin Oncol. 2004;22(19):3909–15.
88. Messina JA, Cheng SC, Franc BL, et al. Evaluation of semi-quantitative scoring system for metaiodobenzylguanidine (mIBG) scans in patients with relapsed neuroblastoma. Pediatr Blood Cancer. 2006;47(7):865–74.
89. Lewington V, Bar Sever Z, Lynch T, et al. Development of a new, semiquantitative I-123 mIBG reporting method in high risk neuroblastoma. Eur J Nucl Med Mol Imaging. 2009;36:334 [abstract].
90. Paltiel HJ, Gelfand MJ, Elgazzar AH, et al. Neural crest tumors: I-123 MIBG imaging in children. Radiology. 1994;190(1):117–21.
91. Bonnin F, Lumbroso J, Tenenbaum F, et al. Refining interpretation of MIBG scans in children. J Nucl Med. 1994;35(5):803–10.
92. Acharya J, Chang PT, Gerard P. Abnormal MIBG uptake in a neuroblastoma patient with right upper lobe atelectasis. Pediatr Radiol. 2012;42(10):1259–62.
93. Schindler T, Yu C, Rossleigh M, et al. False-positive MIBG uptake in pneumonia in a patient with stage IV neuroblastoma. Clin Nucl Med. 2010;35(9):743–5.
94. Okuyama C, Sakane N, Yoshida T, et al. (123)I- or (125)I-metaiodobenzylguanidine visualization of brown adipose tissue. J Nucl Med. 2002;43(9):1234–40.
95. Okuyama C, Ushijima Y, Kubota T, et al. 123I-metaiodobenzylguanidine uptake in the nape of the neck of children: likely visualization of brown adipose tissue. J Nucl Med. 2003;44(9):1421–5.
96. Pfluger T, Schmied C, Porn U, et al. Integrated imaging using MRI and 123I metaiodobenzylguanidine scintigraphy to improve sensitivity and specificity in the diagnosis of pediatric neuroblastoma. Am J Roentgenol. 2003;181(4):1115–24.
97. Melzer HI, Coppenrath E, Schmid I, et al. 123I-MIBG scintigraphy/SPECT versus 18F-FDG PET in paediatric neuroblastoma. Eur J Nucl Med Mol Imaging. 2011;38(9):1648–58.

98. Jacobsson H, Hellstrom PM, Kogner P, et al. Different concentrations of I-123 MIBG and In-111 pentetreotide in the two main liver lobes in children: persisting regional functional differences after birth? Clin Nucl Med. 2007;32(1):24–8.
99. Heyman S, Evans AE, D'Angio GJ. I-131 metaiodobenzylguanidine: diagnostic use in neuroblastoma patients in relapse. Med Pediatr Oncol. 1988;16(5):337–40.
100. Schmiegelow K, Simes MA, Agertoft L, et al. Radio-iodobenzylguanidine scintigraphy of neuroblastoma: conflicting results, when compared with standard investigations. Med Pediatr Oncol. 1989;17(2):127–30.
101. Biasotti S, Garaventa A, Villavecchia GP, et al. False-negative metaiodobenzylguanidine scintigraphy at diagnosis of neuroblastoma. Med Pediatr Oncol. 2000;35(2):153–5.
102. Kushner BH, Yeh SD, Kramer K, et al. Impact of metaiodobenzylguanidine scintigraphy on assessing response of high-risk neuroblastoma to dose-intensive induction chemotherapy. J Clin Oncol. 2003;21(6):1082–6.
103. Hickeson MP, Charron M, Maris JM, et al. Biodistribution of post-therapeutic versus diagnostic (131)I-MIBG scans in children with neuroblastoma. Pediatr Blood Cancer. 2004;42(3):268–74.
104. Parisi MT, Matthay KK, Huberty JP, et al. Neuroblastoma: dose-related sensitivity of MIBG scanning in detection. Radiology. 1992;184(2):463–7.
105. Gordon I, Peters AM, Gutman A, et al. Skeletal assessment in neuroblastoma – the pitfalls of iodine-123-MIBG scans. J Nucl Med. 1990;31(2):129–34.
106. Turba E, Fagioli G, Mancini AF, et al. Evaluation of stage 4 neuroblastoma patients by means of MIBG and 99mTc-MDP scintigraphy. J Nucl Biol Med. 1993;37(3):107–14.
107. Shulkin BL, Shapiro B, Hutchinson RJ. Iodine-131-metaiodobenzylguanidine and bone scintigraphy for the detection of neuroblastoma. J Nucl Med. 1992; 33(10):1735–40.
108. Hadj-Djilani NL, Lebtahi NE, Delaloye AB, et al. Diagnosis and follow-up of neuroblastoma by means of iodine-123 metaiodobenzylguanidine scintigraphy and bone scan, and the influence of histology. Eur J Nucl Med. 1995;22(4):322–9.
109. Zukotynski KA, Fahey FH, Laffin S, et al. Constant ambient temperature of 24 degrees C significantly reduces FDG uptake by brown adipose tissue in children scanned during the winter. Eur J Nucl Med Mol Imaging. 2009;36(4):602–6.
110. Gelfand MJ, O'Hara SM, Curtwright LA, et al. Premedication to block [(18)F]FDG uptake in the brown adipose tissue of pediatric and adolescent patients. Pediatr Radiol. 2005;35(10):984–90.
111. Parysow O, Mollerach AM, Jager V, et al. Low-dose oral propranolol could reduce brown adipose tissue F-18 FDG uptake in patients undergoing PET scans. Clin Nucl Med. 2007;32(5):351–7.
112. Soderlund V, Larsson SA, Jacobsson H. Reduction of FDG uptake in brown adipose tissue in clinical patients by a single dose of propranolol. Eur J Nucl Med Mol Imaging. 2007;34(7):1018–22.
113. Tatsumi M, Engles JM, Ishimori T, et al. Intense (18) F-FDG uptake in brown fat can be reduced pharmacologically. J Nucl Med. 2004;45(7):1189–93.
114. Delbeke D, Coleman RE, Guiberteau MJ, et al. Procedure guideline for tumor imaging with 18F-FDG PET/CT 1.0. J Nucl Med. 2006;47(5):885–95.
115. Shulkin BL, Hutchinson RJ, Castle VP, et al. Neuroblastoma: positron emission tomography with 2-[fluorine-18]-fluoro-2-deoxy-D-glucose compared with metaiodobenzylguanidine scintigraphy. Radiology. 1996;199(3):743–50.
116. Papathanasiou ND, Gaze MN, Sullivan K, et al. 18F-FDG PET/CT and 123I-metaiodobenzylguanidine imaging in high-risk neuroblastoma: diagnostic comparison and survival analysis. J Nucl Med. 2011;52(4):519–25.
117. Colavolpe C, Guedj E, Cammilleri S, et al. Utility of FDG-PET/CT in the follow-up of neuroblastoma which became MIBG-negative. Pediatr Blood Cancer. 2008;51(6):828–31.
118. McDowell H, Losty P, Barnes N, et al. Utility of FDG-PET/CT in the follow-up of neuroblastoma which became MIBG-negative. Pediatr Blood Cancer. 2009;52(4):552 [letter].
119. Goodin GS, Shulkin BL, Kaufman RA, et al. PET/CT characterization of fibroosseous defects in children: 18F-FDG uptake can mimic metastatic disease. Am J Roentgenol. 2006;187(4): 1124–8.
120. Shammas A, Lim R, Charron M. Pediatric FDG PET/CT: physiologic uptake, normal variants, and benign conditions. Radiographics. 2009;29(5): 1467–86.
121. DuBois SG and Matthay KK. ^{131}I-Metaiodobenzylguanidine therapy in children with advanced neuroblastoma. Q J Nucl Med Mol Imaging. 2013;57:53–65.